Automatic arc discharge induced helically twisted long period fiber gratings and its sensing applications

Bing Sun, Wei Wei, Changrui Liao, Lin Zhang, Zuxing Zhang, Ming-Yang Chen, and Yiping Wang

***Abstract*—We experimentally demonstrate an automatic arc discharge technology for inscribing high-quality helically twisted long period fiber gratings (H-LPFGs) with greatly improved inscription efficiency for single mode fibers (SMFs). The proposed technology has been developed by implementing an embedded program in a commercial fusion splicer, which employs an ultraprecision motorized translation stage while the tensioning mass required by conventional inscribing technology is eliminated. More significantly, the arc-induced H-LPFGs have been reported to have potential usage as sensors in temperature, refractive index, twist stress, and strain.**

***Index Terms*—Fiber optics, Fiber optics components, Gratings, Fiber optics sensors.**

I. INTRODUCTION

In recently years, helically twisted long period fiber gratings (H-LPFGs), where a periodicity in the fiber structure is created by homogeneous twisting of a fiber with a noncircular core cross section [1], standard single-mode fibers (SMFs) [2-3], photonic crystal fibers [4-6], or another by creating a helical surface deformation along the fiber [7] have drawn wide attention. Furthermore, the effect of twisting on the propagation of light in the abovementioned optical fibers has been explored for controlling the dispersion, excitation of orbital angular momentum, and elimination of higher-order modes from fiber lasers. For instance, twist characteristics of H-LPFGs have been recently reported [8-10]. The co-directional or contra-directional twist applied to the helix will effectively change the grating period, thus make the resonance wavelength shift towards different directions. Similar to conventional LPFGs, the resonance wavelength also shifts linearly with the applied axial strain [11].

As well known, conventional LPFGs inscribing technologies involved not only UV radiation, CO_2 radiation, and femtosecond laser radiation but also based on ion-beam implantation, etching, mechanical arrangements, acoustic waves, broadband UV light, and electric arc discharges. Among these methods, only the point-to-point direct writing technique by means of a focused CO_2 laser could be utilized to fabricate the H-LPFGs [12]. By contrast, electric arc discharge has paved its way during the past two decades since it is a simple, flexible, and low cost technique that enables the writing of gratings in all kinds of fibers [13-15]. Note that LPFG induced by electric arcs was first demonstrated by Poole et al. [16]. And Yin et al. recently elaborate the irreconcilable contradictions between the quality of the resulting LPFGs and the inscription efficiency in an improved technology, which employs an ultraprecision motorized translation stage, and the tensioning mass required by conventional technology is eliminated [17]. However, to our best knowledge, the H-LPFG induced by electric arc discharge technology has been little investigated.

On the other hand, H-LPFG based sensors have been comprehensively studied and widely used in the fields of civil engineering, industry, biomedicine, and chemistry. More recently, a new method enabling fabrication of HLPGs in a thinned fiber with a diameter smaller than several tens of micrometers has been applied to the refractive index measurements [18]. To be part of LPFG-based sensing systems, the resonant wavelengths of H-LPFGs would be very sensitive to the external temperature, the ambient refractive index, the twisting rate and the applied stress. To some extent, thinned fiber based H-LPFGs combines the performance of SMF based H-LPFGs and tapered fibers. This is because the core diameter of the thinned fiber proportionally changes in accordance with decrement of the cladding diameter. On the other hand, a new kind of thinned fiber based H-LPFGs by means of CO_2 laser has been proposed and developed [18], where a sapphire tube is particularly utilized in place of the focal lens, which thus enables to robustly and repeatedly fabricate H-LPFGs with a

This work was supported by National Natural Science Foundation of China (61505119, 11174064, 61308027, and 61377090), National Postdoctoral Program for Innovative Talents (BX201600077), Brain Gain Foundation of Nanjing University of Posts and Telecommunications (NY215040) and the Key Laboratory of Optoelectronic Devices and Systems of Ministry of Education and Guangdong Province (GD201706).

Bing Sun is with the School of Optoelectronic Engineering, Nanjing University of Posts and Telecommunications, Nanjing 210023, China, and also with Key Laboratory of Optoelectronic Devices and Systems of Ministry of Education and Guangdong Province, Shenzhen University, 518060, China (e-mail: b.sun@njupt.edu.cn).

Zuxing Zhang, Wei Wei are with the School of Optoelectronic Engineering, Nanjing University of Posts and Telecommunications, Nanjing 210023, China (e-mail: zxzhang@njupt.edu.cn; weiwei@njupt.edu.cn).

Changrui Liao, Yiping Wang are with the Key Laboratory of Optoelectronic Devices and Systems of Ministry of Education and Guangdong Province, College of Optoelectronic Engineering, Shenzhen University, Shenzhen 518060, China (e-mail: cliao@szu.edu.cn, ypwang@szu.edu.cn).

Lin Zhang is with the Aston Institute of Photonic Technologies, Aston University, Birmingham B4 7ET, UK (e-mail: l.zhang@aston.ac.uk).

Ming-Yang Chen is with the Institute of Opt-Electronics and Communication Technologies, Jiangsu University, Zhenjiang 212013, Jiangsu Province, China (e-mail: miniyoung@163.com)

high quality. Furthermore, the proposed method allows fabrication of H-LPFGs with a diameter less than several tens of micrometers.

In this Letter, we first employ a commercial fusion splicer system (ARC Master FSM-100P, Fujikura) to inscribe H-LPFGs in the conventional SMFs. As shown in Fig. 1, the H-LPFG is distinguished in the refractive index modulation of a helical structure such as a screw. Two cleaved standard SMFs clamped by the left and right holders of the splicer are spliced before performing the automatic H-LPFG inscription process which we implemented in the splicer system beforehand. Then, it will be stopped once a desired H-LPFG transmission spectrum is obtained based on periodical monitoring of the transmission spectrum using an broadband ASE source and an optical spectral analyzer (AQ6370C, Yokogawa Electric Corp.) with a wavelength resolution of 20 pm. The transmission spectrum of the H-LPFG displays several dips that correspond to coupling of light from the core mode to the cladding modes. Schematic diagram of the microscopic image of the H-LPFG is shown in the left inset. Furthermore, the arc-induced H-LPFG has been reported to have potential usage as sensors in temperature, refractive index, twist stress, and strain.

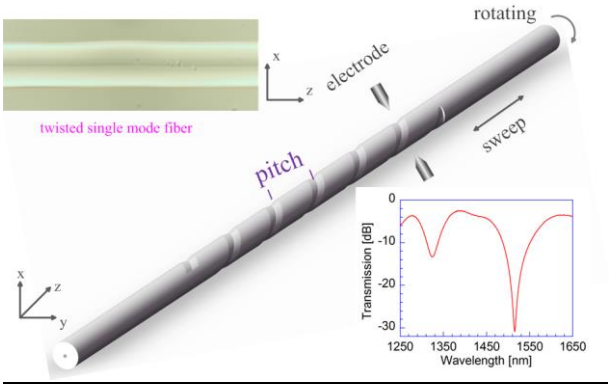

Fig. 1. The schematic of a helical long period fiber grating (H-LPFG). The insets show side view of the H-LPFG with periodic twisting and the transmission spectrum of the fabricated H-LPFG, respectively.

II. Device Fabrication

Generally, the H-LPFG could also be described by the conventional coupled-mode theory between the core and the cladding modes. The period of the H-LPFG is equal to the pitch of helix, which can be calculated by [19]

$$\Lambda_g = L/N \quad (1)$$

where $\Lambda_g$is period of H-LPFG, L is the length of the twisted fiber section, and N is the number of twist turns. Similar to conventional LPFGs, H-LPFGs couple the guided fundamental mode to forward-propagating cladding modes. For the single-helix H-LPFG in a conventional SMF, the phase-matching condition can be described as [20]

$$\lambda_i = (n_{core} - n_{clad}^i)\Lambda_g \quad (2)$$

where n_{core} is the effective refractive index of fundamental mode, n_{clad}^i is effective refractive index of i-order cladding mode, Λ_g is the period of the grating, and λ_i is the resonance wavelength of the grating.

Fig. 2. (a) Photograph of the arc discharge technology employing a commercial fusion splicer (FSM-100P); (b) first step (discharge); (c) second step (move fiber); (d) third step (jump).

The automatic H-LPFG inscription program involves two motors, namely, θ_L, and SWEEP motors, which is comprised of the three main parts illustrated in Fig. 2. As shown in Fig. 2 (c), one part involves θ_L motor, with the twist speed, e.g., V_θ=40 degree/s in this program, which determine the required time for rotating a period is 9 s. Another is to move the fiber according to the grating pitch (Λ) and the period, e.g., Λ=450 μm and N=16, respectively, along its longitudinal axis via the SWEEP motor, as shown in Fig. 2(d). Here, the grating pitch is determined by multiplying the Finish Time by the Initial Speed, e.g., V=50 μm/s. Furthermore, accompanied part is performing arc discharge for N periods of time, e.g., 146 s, as shown in Fig. 2(b). The arc discharge time is determined by subtracting the Start Time from the Finish Time. We analyzed the influence of the arc current on the grating growth for the SMF by inscribing several gratings with the same grating pitch and concluded that high-quality H-LPFGs in SMFs could be achieved when the arc current is fixed at STD-2.6 mA. It should be noted that fabricating LPFGs by use of arc discharge technology belong to high reproducibility [17]. As a result, the program is automatically executed by pushing the button labeled SET on the splicer panel and stopped by pushing the button labeled RESET. Furthermore, the program is transferable to any FSM-100 series splicer for the H-LPFG inscription. We have fabricated two H-LPPFG samples with different values of Λ in order to verify the feasibility of arc discharge inscribing technology. It can be seen from Fig. 3 that the gratings exhibited good quality with clean spectra, the depth of the resonant peaks closed to 30 dB, and low insert losses of ~2 dB.

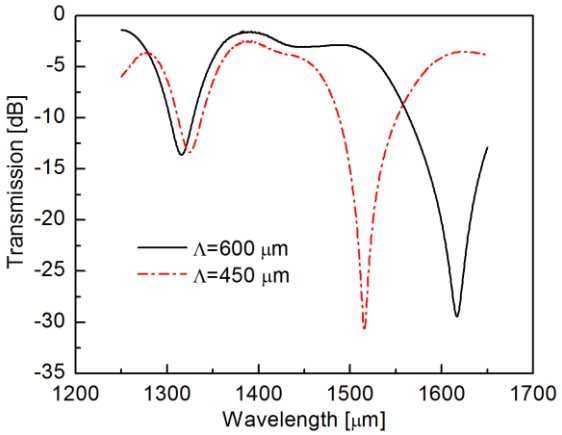

Fig. 3. Transmission spectra of H-LPFGs inscribed in SMF with different grating pitch.

We all know that the fiber transmission spectra are determined by the helix pitch Λ_g. In the meanwhile we detailed that the automatic H-LPFG inscription program involves two motors, namely, θ_L, and SWEEP motors. However, the twist speed V_θ could range from 1 degree/s to 50 degree/s, as shown in Fig. 4(a), and the speed of the SWEEP motor could range from 10 μm/s to 1000 μm/s, as shown in Fig. 4(b). So the required time for rotating a period is equal to 360 degree divided by V_θ. As a result, the helix pitch Λ_g is determined by multiplying the required time for rotating a period by the SWEEP speed V.

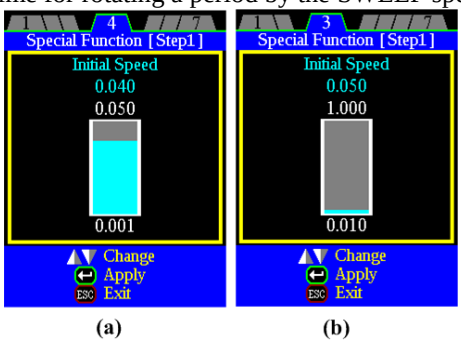

Fig. 4. The twist speed V_θ could range from 1 degree/s to 50 degree/s (a) and the speed of the SWEEP motor could range from 10 μm/s to 1000 μm/s (b).

III. Experimental Result and Discussion

We have first investigated the responsivities of the H-LPFG for the temperature with an ASE source and an optical spectrum analyzer in our experiment. To investigate the thermal performance, the H-LPFG was first placed in a column oven, where the temperature can be discretely changed from 20 ℃ to 100 ℃ with a resolution of 0.1 ℃. The measured results were shown in Fig. 5. As the temperature was increased, the spectrum was linearly shifted to the long-wavelength direction with a responsivity of ~70 pm/ ℃, which is almost the same level as that reported in [12].

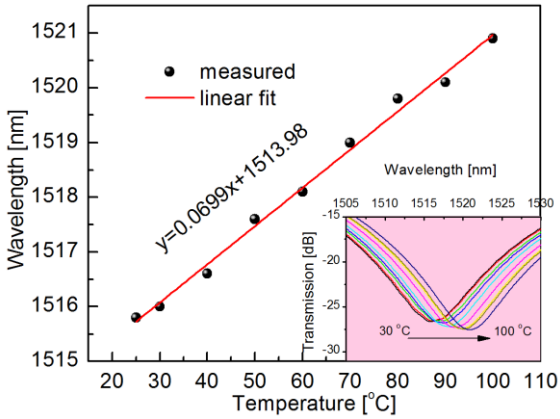

Fig. 5. Dependence of the resonance wavelength on temperature.

To characterize the refractive index (RI) performance, a set of refractive index matching liquids (Cargille Labs, http://www.cargille.com/) with a RI from 1.40 to 1.45 was employed. Such refractive index matching liquids were employed as the ambient solutions, which were filled around the ambient region of the H-LPFG. Meanwhile, the temperature remained at a room temperature. Figure 6 shows the measuring results for the transmission spectra of the H-LPFG. It was found that as the refractive index was increased, the two loss peaks began to shift to the short wavelength direction, i.e. 'blue' shift. The curve is fit by exponential function with a high goodness-of-fit coefficient R^2 value.

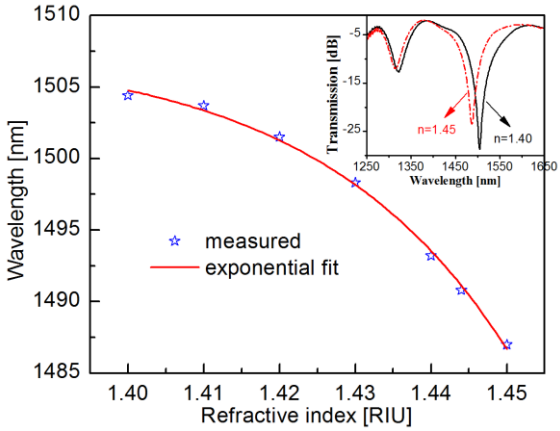

Fig. 6. Resonant wavelength shift of the H-LPFG at different surrounding RIs. The inset shows the transmission spectra of the proposed device immersed in the liquids with a RI of 1.40 and 1.45.

Fig. 7 shows that the experimental results when the co-direction and contra-direction twist stress were applied on the H-LPFG, respectively. The inset showed the transmission spectra of the SMF-HLPG. It indicated the response of the resonance shift and corresponding grating contrast of the H-LPFG to the applied twist. It was found that the resonance wavelength shifts linearly towards longer wavelength when co-directional twist was applied and the opposite process occurred when contra-direction twist was applied. The contrary behavior agreed with the theoretical analysis. The resonance wavelength (~1515 nm) of the H-LPFG varied monotonically and linearly with a sensitivity of -46.46 nm/(rad/mm), which is an order magnitude higher than that of the conventional CO_2-laser written LPFGs [12]. The grating contrast decreased when the

twist was applied on the H-LPFG, which can be attributed to the decrease of coupling coefficient caused by the torsion [21].

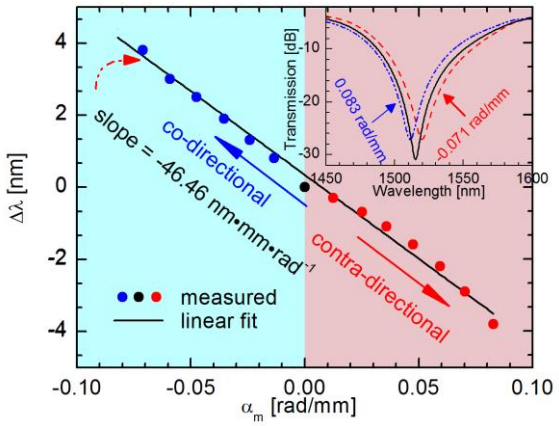

Fig. 7. (a) Resonance wavelength versus twist rate. The inset is the transmission spectra of the H-LPFG.

We also investigated the responses of the H-LPFG to the applied tensile strain. First, one end of the H-LPFG was fixed, and another end was attached to a translation stage with a resolution of 10 μm. The total length of the stretched fiber, including the SMF and the grating, was 190 mm. The wavelength shift of the interference fringe around 1515 nm was measured while the tensile strain was increased from 0 to 480 με with a step of 50 με. As shown in Fig. 8, the dip wavelength of the resonant wavelength of the H-LPFG sample shifted linearly toward a longer wavelength with the increased tensile strain. Providing an optical spectrum analyzer with a resolution of 0.02 nm was employed, a strain sensitivity of 1.88 pm/με could be achieved. Additionally, the minimum intensity of interference fringe, i.e. dip intensity, exponentially increased while the applied tensile strain was increased from 0 to 500 με.

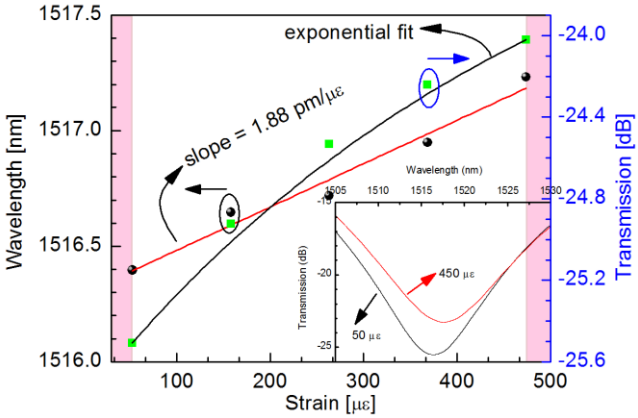

Fig. 8. Measured shift in resonance wavelength as a function of axial strain.

IV. Conclusion

In conclusion, a promising arc discharge technology was proposed for fabricating H-LPFGs with the improved quality and inscription efficiency, where a preset automatic program in a commercial fusion splicer using two fiber holders rather than a single holder and a tensioning mass was implemented. It is possible to tailor the resonant dip by simply adjusting the temperature, ambient refractive index, twist rate and axial strain. Automatically, it has potential usage as sensors. However, this elaborate work is still in progress. Moreover, potential applications are in nonlinear chiro-optical effects, polarization control, filtering, microscopy, and spectroscopy. Note that we have not made the analysis of polarization characteristics of the fabricated H-LPFG due to limited experimental devices.

References

[1] V. I. Kopp, V. M. Churikov, J. Singer, N. Chao, D. Neugroschl, and A. Z. Genack, "Chiral fiber gratings," Science 305(5680), 74-75 (2004).
[2] S. Oh, K. R. Lee, U. C. Paek, and Y. Chung, "Fabrication of helical long-period fiber gratings by use of a CO2 laser," Opt. Lett. 29(13), 1464-1466 (2004).
[3] C. Jáuregui and J. M. López-Higuera, "Virtual long-period gratings," Opt. Lett. 30(1), 14-16 (2005).
[4] A. Michie, J. Canning, I. Bassett, J. Haywood, K. Digweed, M. Åslund, B. Ashton, M. Stevenson, J. Digweed, A. Lau, and D. Scandurra, "Spun elliptically birefringent photonic crystal fibre," Opt. Express 15(4), 1811-1816 (2007).
[5] A. Argyros, J. Pla, F. Ladouceur, and L. Poladian, "Circular and elliptical birefringence in spun microstructured optical fibres," Opt. Express 17(18), 15983-15990 (2009).
[6] G. K. L. Wong, M. S. Kang, H. W. Lee, F. Biancalana, C. Conti, T. Weiss, and P. St. J. Russell, "Excitation of Orbital Angular Momentum Resonances in Helically Twisted Photonic Crystal Fiber," Science 337, 446-449 (2012).
[7] W. Shin, B. A. Yu, Y. C. Noh, J. Lee, D. K. Ko, and K. Oh, "Bandwidth-tunable band-rejection filter based on helicoidal fiber grating pair of opposite helicities," Opt. Lett. 32(10), 1214-1216 (2007).
[8] X. Xi, G. K. L. Wong, T. Weiss, and P. S.J. Russell, "Measuring mechanical strain and twist using helical photonic crystal fiber," Opt. Lett., 38(24), 5401-5404 (2013).
[9] R. Gao, Y. Jiang, and L. Jiang, "Multi-phase-shifted helical long period fiber grating based temperature-insensitive optical twist sensor," Opt. Express 22(13), 15697-15709 (2014).
[10] L. L. Xian, P. Wang, and H. P. Li, "Power-interrogated and simultaneous measurement of temperature and torsion using paired helical long- Period fiber gratings with opposite helicities," Opt. Express 22(17), 20260-20267 (2014).
[11] L. Zhang, Y. Liu, Y. Zhao, T. Wang, "High Sensitivity Twist Sensor Based on Helical Long-Period Grating Written in Two-Mode Fiber," IEEE Photon. Technol. Lett., 28(15), 1629-1632 (2016).
[12] Y. Rao, Y. Wang, Z. Ran, and T. Zhu, "Novel fiber-optic sensors based on long-period fiber gratings written by high-frequency CO_2 laser pulses," J. Lightwave Technol. 21(5), 1320-1327 (2003).
[13] A. Iadicicco, S. Campopiano, A. Cusano, "Long-Period Gratings in Hollow Core Fibers by Pressure-Assisted Arc Discharge Technique," IEEE Photon. Technol. Lett. 23(21), 1567-1569 (2011).
[14] G. Rego, P. V. S. Marques, J. L. Santos, and H. M. Salgado, "Arc-induced long-period gratings," Fiber Integr. Opt. 24, 245-259 (2005).
[15] A. Martinez-Rios, I. Torres-Gomez, D. Monzon-Hernandez, G. Salceda-Delgado, V. M. Duran-Ramirez, and G. Anzueto-Sanchez, "Random period arc-induced long-period fiber gratings," Opt. Laser Technol. 44, 1176-1179 (2012).
[16] C. D. Poole, H. M. Presby and J. P. Meester, "Two-mode fibre spatial-mode converter using periodic core deformation", Electron. Lett. 30(17), 1437-1438 (1994).
[17] G. Yin, J. Tang, C. Liao, and Y. Wang, "Automatic arc discharge technology for inscribing long period fiber gratings," Appl. Opt. 55(14), 3873-3878 (2016)
[18] P. Wang and H. Li, "Helical long-period grating formed in a thinned fiber and its application to a refractometric sensor," Appl. Opt. 55(6), 1430-1434 (2016).
[19] C. D. Pool, C. D. Townsend and K. T. Nelson, "Helical-grating two-mode fiber spatial-mode coupler", J. Lightwave Technol. 9(5), 598-604 (1991).
[20] Oleg V. Ivanov, "Propagation and coupling of hybrid modes in twisted fibers," J. Opt. Soc. Am. A 22, 716-723 (2005).
[21] L. Zhang, Y. Liu, Y. Zhao, and T. Wang, "High Sensitivity Twist Sensor Based on Helical Long-Period Grating Written in Two-Mode Fiber," IEEE Photon. Technol. Lett. 28(15), 1629-1632 (2016).